Compressive strength and microstructure of ordinary cured and autoclaved cement-based composites with mechanically activated kaolins

Biljana Ilić[a*], Aleksandra Mitrović[a], Ljiljana Miličić[a], Miodrag Zdujić[b], Miroslava Radeka[c]

[a] *Institute for Testing of Materials, Bulevar vojvode Mišića 43, 11000 Belgrade, Serbia*

[b] *Institute of Technical Sciences of the Serbian Academy of Sciences and Arts, Knez Mihailova 35, 11000 Belgrade, Serbia*

[c] *Faculty of Technical Sciences, University of Novi Sad, Department of Civil Engineering, Trg Dositeja Obradovića 6, 21000 Novi Sad, Serbia*

[*]*Corresponding author: biljana.ilic@institutims.rs, Bulevar vojvode Mišića 43, 11000 Belgrade, Serbia*

Abstract

The effects of two different mechanically activated kaolins, AKV (61% kaolinite, 14% quartz and 16% mica) and AKG (51.6% kaolinite and 40.6% quartz) on the compressive strength of cement composites and microstructure of pastes were investigated. Composite mixtures, in which 10, 20, 30, 40 and 50% of ordinary Portland cement (OPC) was replaced by AKV or AKG, were prepared with w/b of 0.5, and exposed to different curing conditions (ordinary curing for 28 days and autoclaving). Factors affecting microstructure were investigated on pastes by X-ray diffraction (XRD), Differential thermal analysis/thermal gravimetry (DTA/TG) analyses, Mercury intrusion porosimetry (MIP) and Scanning electron microscopy with Energy-dispersive spectroscopy (SEM-EDS).

AKG composites exhibited higher compressive strengths under both curing conditions. Positive autoclaving effects on strengths were predominantly pronounced at the higher cement replacement levels. Comparison of the autoclaved and ordinary cured paste microstructure, revealed more intensive pozzolanic reaction during autoclaving conditions (CH content near zero) and higher total porosity. The negative effect of hydrogarnet on the strength was compensated by the formation of the crystalline tobermorite.

Obtained results revealed that mechanically activated kaolin, with high content of quartz, could be a promising pozzolanic addition, even at high cement replacement levels (30–50%), especially when autoclaving curing conditions were applied.

Keywords: mechanically activated kaolin; cement-based composites, microstructure, ordinary curing, autoclave curing

1. Introduction

Pozzolanic additions, as supplementary cementitious materials (SCMs), are widely used for substitution clinker in cement, or cement in mortars or concretes. They could be by origin natural or artificial [1]. There are two types of artificial pozzolanic additions: byproducts, such as fly ash and silica fume, and thermally activated clays, whereby the best known is metakaolin (MK).

Pozzolanic additions are used to improve technical characteristics of mortars and concretes, such as strength, durability, rheological and transfer properties. The enhancement of these properties is related to the reactivity (chemical pozzolanicity), as their additions lead to a formation of supplementary cementitious compounds (SCCs), but also to their fineness (physical pozzolanicity) [2]. Beside technical benefits, their use reduces energy consumption and has environmental benefits as a result of reduction in the carbon dioxide emission, compared to the manufacture of Portland cement [3],[4].

MK, commercially produced from 1990, is manufactured under stringent conditions from a selected naturally occurring kaolin. The industrial process generally comprises selection/grinding, then thermal activation/calcination of the raw kaolin for several hours in a rotary kiln, followed by grinding of the burned material. The quality and reactivity of MK is strongly dependent on the composition and structure of the kaolin used, and on the thermal activation efficiency to remove chemically-bound water, through dehydroxylation [5], [6], [7]. Complete dehydroxylation corresponds to the destruction of kaolinite crystallinity (amorphisation) resulting in an increase of pozzolanic activity.

Supplies of traditional SCMs (fly ash, blast furnace slag, silica fume) are quite limited compared to the worldwide production of cement. However, nowadays application of MK, due to its high price is limited to high-strength or high-performance concretes. Increased demand for additions, which might substitute traditional SCMs and might be produced at lower cost, led to many investigations of alternative pozzolanic additions. One of the alternative pozzolana is mechanically activated kaolin. Although many studies [8], [9], [10], [11] have shown benefits of mechanical activation of kaolin, this process, as far as we know,

has not been yet applied on the industrial scale. Several studies showed that the optimization of the milling method and consumed energy, could be an additional tool for kaolin modification and production [12], [13], [14], [15].

MK is used in various types of ordinary cured concrete, such as high-performance concrete, high-strength and lightweight concrete, glass fibre reinforced concrete [16]. In order to improve properties of concrete with MK, at least 15–20% of cement has to be replaced. The optimum replacement level of cement with MK is dependent on the nature and proportion of different reaction products, temperature and reaction time. Literature review [17] shows that optimal performance of concrete is achieved by replacing 10% to 15% of the cement with MK. While it is possible to use less amount, the benefits are not fully realized until at least 10% of MK is used. Compressive strength of concrete with MK after 28 days of curing could be 20% higher compared to the reference concrete.

Recent studies [18], [19] have demonstrated that beside ordinary curing conditions, MK could be used under steam-curing, usually applied in the precast industry. Studies showed that it was possible to substitute up to 25% of cement with MK, whereby positive effects on the strength were still achieved.

Although the reactivity of mechanically activated kaolin is similar or slightly inferior to that of thermally activated kaolin, there are few publications [11], [20], [21] referring to its utilization in cement composites. Also, a general description of the effect of mechanochemically activated kaolinite on the hydration reactions and properties of cement-based composites is lacking. Therefore, the investigation of strength, hydration products, microstructure and other performance parameters of cement-based composites containing mechanically activated kaolins is considered important.

This research is the continuation of our previous investigation [20], [22], [23] with the main objective to enlarge the use of mechanically activated kaolins in cement-based systems. Its main objective is to show how the use of two different mechanically activated kaolins affects strength and microstructure of cement composites, cured under different conditions.

2. Materials and methods

2.1. Raw materials

Two different mechanically activated kaolins, AKV and AKG, were used for cement replacement. Their main physical and chemical properties are presented in Table 1. The complete details about activation conditions can be obtained elsewhere [20], [24]. AKV was obtained from kaolin having 61% of kaolinite, 14% of quartz and 16% mica, while major minerals in AKG were kaolinite 51.5% and quartz 40.6%.

Table 1. Properties of AKV and AKG

	AKV [20]	AKG [24]
Pozzolanic activity, MPa	13.7	14.0
Reactive silica content, %	29.52	33.00
Specific surface area, m^2/g	49.76	21.75
Particle size (d_{50}), μm	5.913	6.346

Ordinary Portland cement (OPC), CEM I 42.5R, produced by Lafarge BFC, Beočin Serbia with a Blaine fineness of 4120 cm^2/g, and the following chemical composition (mass %): SiO_2 20.86, Al_2O_3 5.59, Fe_2O_3 2.49, CaO 62.40, MgO 2.50, K_2O 0.77, Na_2O 0.22, SO_3 3.63 and LOI 1.74, was used.

CEN Standard sand, distilled water, superplasticizer Sika ViscoCrete TECHNO 20S and hydrated lime were also used.

2.2. Design, mixing, curing and testing

2.2.1. Composite mixtures

Composite mixtures, where 10%, 20%, 30%, 40% and 50% of cement was replaced with AKV or AKG, were prepared with the water-to binder ratio 0.50, and the sand to binder ratio 3.0. For the purpose of comparison, also a reference mix (Ref. C) having only OPC as the binder was studied. The workability was adjusted using superplasticizer. Hydrated lime was added at higher cement replacement levels - 30%-50% (designation CH) in order to secure enough CH for pozzolanic reaction. For estimation of the hydrated lime quantity it was assumed that 20% of CH was released during the cement hydration, and that the best mechanical properties could be achieved when MK was reacted with CH in the ratio MK/CH = 2 [1], [25].

112 Composite mixture proportions are presented in Table 2.

113 *Table 2. Composite mixture proportions*

Designation	Cement, (g)	Mechanically activated kaolin, (g)	Sand, (g)	Water, (ml)	Superplasticizer, (ml)	Slump, (mm)
Ref.C	450	-	1350	225	-	164
AKV 10	405	45	1350	225	-	158
AKV 20	360	90	1350	225	1.50	157
AKV 30 CH	315	135	1350	225	3.32	159
AKV 40 CH	270	180	1350	225	6.10	156
AKV 50 CH	225	225	1350	225	9.40	160
AKG 10	405	45	1350	225	-	178
AKG 20	360	90	1350	225	-	184
AKG 30 CH	315	135	1350	225	-	173
AKG 40 CH	270	180	1350	225	0.75	160
AKG 50 CH	225	225	1350	225	3.01	157

114 The specimens were cast in moulds (three prisms size 40 x 40 x 160 mm) using vibration
115 table.

116 *2.2.2 Curing*

117 In order to examine the effects of curing conditions on the mechanical properties of
118 composites, ordinary and autoclave curing were applied.

119 Samples were stored in the mould in the moist atmosphere for 24 h and thereafter hardened
120 samples were ordinary cured in water under standard curing conditions until the testing age
121 of 28 days, or autoclave cured at constant temperature and pressure of 216 ^{o}C and 2 MPa
122 for 4 h. Then the autoclave heater was turned off and the chamber was allowed to cool
123 naturally.

124 *2.2.3. Compressive strength test*

125 Compressive strength measurements were carried out according to EN 196-1.

126 *2.2.4.Cement paste*

127 Representative pastes with 20% (AK 20) and 30% and 50% of AKV or AKG, with the addition
128 of appropriate hydrated lime quantity (AK 30 CH and AK 50 CH), were prepared, with water-
129 to-binder ratio (w/b) of 0.4, for determination of hydration products and for measurements of

130 porosity and pore size distribution. Ordinary cement paste (without AK) was prepared as the
131 reference (Ref. P).
132 Paste samples were cast in cubic moulds (50 mm x 50 mm x 50 mm), and cured in the same
133 way as composite mixtures. The hydration reaction was stopped at 28 days by immersing
134 crushed particles in acetone for 24 h to replace free water. Afterwards, the samples were
135 subjected to drying at 65 ^{o}C in an oven for 24 h. The pretreated fractured samples were
136 analyzed by mercury intrusion porosimeter and scanning electron microscopy coupled with
137 EDS detector.
138 Samples for determination of hydration products were additionally milled for 60 s in the
139 oscillatory Herzog HSM 100 mill, to pass 45 μm sieve.
140 *2.2.5. Microstructure testing*
141 The following techniques were used for the evaluation of microstructure of pastes:
142 ▪ X-Ray Diffraction (XRD) analysis for the identification of crystalline phases in pastes
143 (Philips PW 1050 diffrectometer, with 40 kV and 30 mA, using Cu-Kα graphite-
144 monochromatized radiation (λ=1.5418 A)). Data were recorded from 5° to 60° 2θ, with
145 the step size of 0.05° and time per step of 10 s. Crystalline phases were identified
146 using EVA software package v.9.0 and PDF-2 database.
147 ▪ Differential Thermal and Thermogravimetric Analysis (SDT Q600 simultaneous
148 TG/DTA instrument (TA Instruments)) were performed under dynamic (100 cm^3 min^{-1})
149 N_2 atmosphere, with a heating rate of 20 °Cmin^{-1}, from ambient temperature up to
150 1100 °C, in order to investigate the $Ca(OH)_2$ consumption and to determine the
151 hydration reaction products.
152 ▪ Mercury intrusion porosimetry (MIP) tests for the microstructural determination of total
153 porosity and pore size distribution were performed on the AutoPore IV 9500 mercury
154 porosimeter with a maximum 228 MPa injection pressure.
155 ▪ The morphology of hydration products of selected pastes was observed by scanning
156 electron microscopy (SEM) using a JEOL JSM-6460 LV coupled with EDS detector

(LINK AN 1000 EDS microanalyzer). The samples were coated with gold and the SEM-EDS analysis was carried out at an accelerating voltage of 20 kV.

3. Results and discussion

3.1 Compressive strength

The effect of substitution of OPC by AKV or AKG on the compressive strengths of composites ordinary cured for 28 days or autoclaved is presented in the Fig. 1.

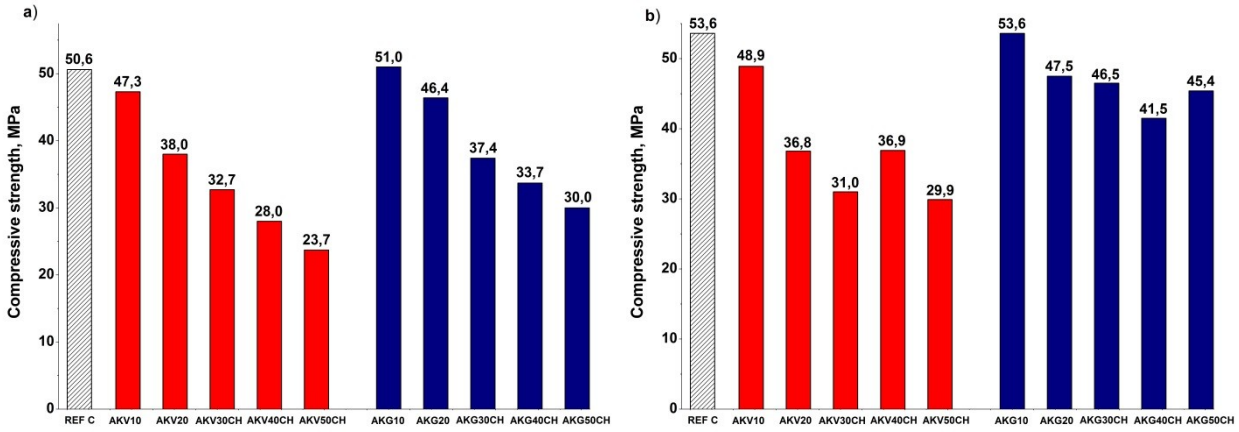

Figure 1. Compressive strengths of composites: a) ordinary cured for 28 days, (b) autoclaved

AKG composites had higher compressive strengths for all cement replacement levels under the both curing conditions compared to the AKV composites.

Strengths of ordinary cured composites with both mechanically activated kaolins continually decreased with a higher cement replacement level. A tendency of decreasing strength was similar to the calculated values assuming that only dilution effect affected the strength. Only the strength of AKG 10 composite was higher than that of the reference.

Autoclaving the reference mixture and composites with 10% and 20%, either AKV or AKG, led to small strength changes, compared to the ordinary cured composites. AKG 10 composite had the same strength as the reference, while the strength of composites with 20% AKG was about 10% lower. Also, results show that when AKG is used, cement could be replaced in higher percentage. Autoclaving the composites with over 30% of mechanically activated kaolin, significantly increased strengths, compared to ordinary curing. This effect is particularly pronounced in AKG composites. Very good results were obtained for a composite with 50% of AKG, for which relative strength was about 85%.

The results confirmed conclusions given in the studies [26], [27], [28] that under autoclaving conditions, presence of crystalline quartz had a positive effect on the mechanical properties. The ~~positive~~ effect of quartz at elevated temperature and pressure was explained by the reaction between activated crystalline quartz and portlandite [29], which produced more crystalline C-S-H products with lower Ca/Si such as tobermorite or xonotlite [30]. Another contribution of fine quartz crystals is that they became nuclei for the formation of crystalline products [31].

3.2 XRD analysis

Crystalline phases identified in AKV and AKG pastes under different curing conditions are presented in Fig. 2.

3.2.1 XRD of ordinary cured

Several major crystalline minerals are detected in reference paste ordinary cured: alite (C_3S) and belite (C_2S), originated from non-hydrated cement, and portlandite (CH), as the cement hydration product [32] (Eq.1.).

$$C_3S + C_2S + H \rightarrow C\text{-}S\text{-}H + CH \quad (1)$$

(Portland cement)

Addition of mechanically activated kaolin caused formation of additional crystalline minerals, compared to the reference paste.

In AKV pastes ettringite ($C_6A\dot{S}_3H_{32}$) and tetracalcium aluminate hydrate (C_4AH_{13}) were detected. Ettringite was formed during cement hydration, while the tetracalcium aluminate hydrate appeared as a product of reaction between alumina from pozzolanic material and portlandite (Eq 2.) [2].

$$Pozzolan + CH + H \rightarrow SCCs\ (C\text{-}S\text{-}H;\ C\text{-}A\text{-}H;\ C\text{-}A\text{-}S\text{-}H) \quad (2)$$

Kaolinite ($Al_2Si_2O_5(OH)_4$) peaks, present in AKV pastes, arising from non-amorphized kaolinite, left behind after mechanical activation [33], while the quartz (SiO_2) reflections, detected as a minor phase, originated from impurities. The intensity of quartz peaks increased with a higher cement replacement level. A slight reduction of portlandite peaks, compared to the reference paste, indicated weak pozzolanic reaction.

206 In AKG pastes, besides ettringite and tetracalcium aluminate hydrate, new crystalline phase -
207 strätlingite (C_2ASH_8) was formed by the pozzolanic reaction (Eq 2.). The presence of CH
208 peaks indicates that its content was over quantity needed to bind pozzolan in the reaction.
209 The results are opposite to the conclusions given in research [34] where authors stated that
210 the simultaneous presence of both strätlingite and portlandite was impossible. The
211 tetracalcium aluminate hydrate and ettringite peaks were more pronounced, compared to
212 those in AKV pastes.
213 Higher strengths gained in ordinary cured AKG composites mainly arised from the absence
214 of kaolinite peaks and higher consumption of CH in pozzolanic reaction, which led to an
215 increased content of C-S-H phases.
216 *3.2.2 XRD of autoclaved*
217 The difference between autoclaved and ordinary cured reference paste is in appearance of
218 jaffeite, which is in accordance with findings [35] that the main hydration product C–S–H gel,
219 formed at elevated temperature and pressure, transforms to α-C_2SH (crystalline α-dicalcium
220 silica hydrate) or $C_3SH_{1.5}$ (C_3S hydrate or jaffeite) according to the Eq. 3.
221 $C_3S + C_2S + H \rightarrow$ C-S-H + CH $\rightarrow$ C-S-H (α-C_2SH, $C_3SH_{1.5}$) (3)
222 (Portland cement)
223 In autoclaved AKV pastes the following phases were detected: tobermorite ($C_5S_6H_5$),
224 hydrogarnet (C_3ASH_4), kaolinite, quartz and portlandite.
225 Tobermorite was formed in the reaction between crystalline calcium silica hydrates (*α*-C_2SH,
226 $C_3SH_{1.5}$) and reactive silica from pozzolana, by Eq 4. [35], [36]. The formed tobermorite filled
227 the pores and enhanced the compactness of the composites.
228 C-S-H + CH + $SiO_2^R \rightarrow C_5S_6H_5$ (4)
229 The presence of Al_2O_3, arising from mechanically activated kaolin, also affected the structure
230 and nature of hydration products. The small amount of Al_2O_3 resulted in the formation of Al-
231 substituted tobermorite, but as the Al amount increased, hydrogarnet was formed [36], [37]
232 according to Eq. 5, which resulted in a strength decrease.
233 $C_3A + C_2(A,F) \rightarrow (C_3ASH_4)$ (5)

Presence of kaolinite, quartz and portlandite might be explained in the same manner as for ordinary cured AKV pastes.

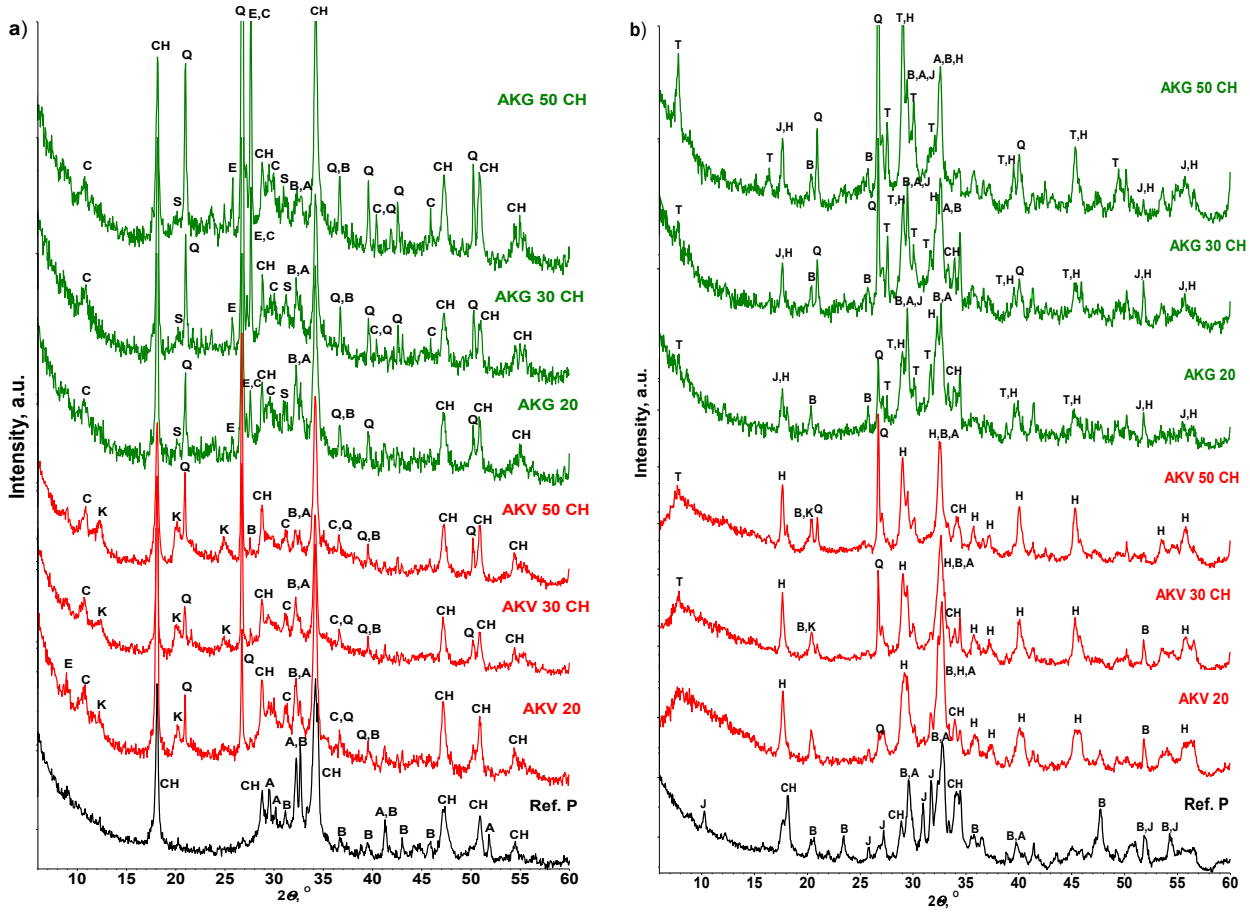

Fig 2. The XRD paterns of pastes a) ordinary cured for 28 days b) autoclaved (A – alite, B – belite, CH – portlandite, E – ettringite, C - tetracalcium aluminate hydrate, K – Kaolinite, Q - Quartz, S - strätlingite, J - jaffeite, T - tobermorite, H - hydrogarnet)

AKG autoclaved pastes were characterized by the presence of jaffeite, tobermorite, hydrogarnet, quartz and portlandite. Absence of kaolinite peaks and low intensity of portlandite peaks indicated that CH was almost completely consumed in pozzolanic reaction. Tobermorite peaks were more pronounced at AKG pastes compared to the AKV pastes, while hydrogarnet peaks were lower and usually overlapped with jaffeite. These could be explained by the fact that at elevated temperatures and pressures, finely milled quartz particles from AKG, participated in the pozzolanic reaction forming crystalline tobermorite, as a main reaction product. These results confirms findings [26], [27], [28], [30], as well as the fact that the presence of the crystalline quartz resulted in higher strengths.

3.3 DTA/TG analysis

DTA and TG curves of the ordinary cured and autoclaved pastes are given in the Figs. 3 and 4, respectively.

3.3.1 DTA of ordinary cured

DTA curves of ordinary cured AKV and AKG pastes were very similar to the reference paste, implying similar thermal behavior during heating to 1000 ^{o}C. The broad endothermic peak in temperature range up to 250 °C was attributed to the loss of free moisture as well as to the dehydration of calcium silicate hydrates (C-S-H). According to the literature [19], [32], [34], [38], this peak might overlap with the peak from decomposition of ettringite and monosulfoaluminate hydrates.

The endothermic peak between 400 and 500 ^{o}C originated from dehydroxylation of CH [39], [40]. Small peaks at ~170 °C and ~280 °C may be attributed to the decomposition of strätlingite [38], [41] and tetracalcium aluminate hydrate, respectively [42], [43], while exothermic peak above 800 ^{o}C is due to the crystallization of unreacted amorphous kaolin.

3.3.2 DTA of autoclaved

In comparison to ordinary cured, autoclaved pastes exhibit remarkably different thermal behavior. The main difference is in formation of new phases, such as hydrogarnet, Al-substituted tobermorite, wollastonite ($CaSiO_3$) and anorthite ($CaAl_2Si_2O_8$), which may be revealed at DTA curves of autoclaved pastes (Fig. 3b).

As can be seen, pronounced broad peak of C-S-H at ~155 °C [44], [45], which is characteristic for all ordinary cured pastes is very weak for reference sample, but becomes more pronounced in AK pastes, especially in AKG pastes.

The endotherms at ~310 °C and ~360 °C, arise from the dehydration of hydrogarnet [46], [47]. These peaks become significantly wider in pastes with higher content of AKV and in the paste AKV 50 CH they merge in one peak. The hydrogarnet peaks were more pronounced in AKV pastes.

Characteristic peak of CH dehydroxylation appears at ~440 °C for reference paste, but almost vanish for AKV 20, AKV 30 CH and AKG 30 CH pastes, as a result of pozzolanic reaction. However, it may be identified in AKV 50 CH and AKG 50 CH pastes.

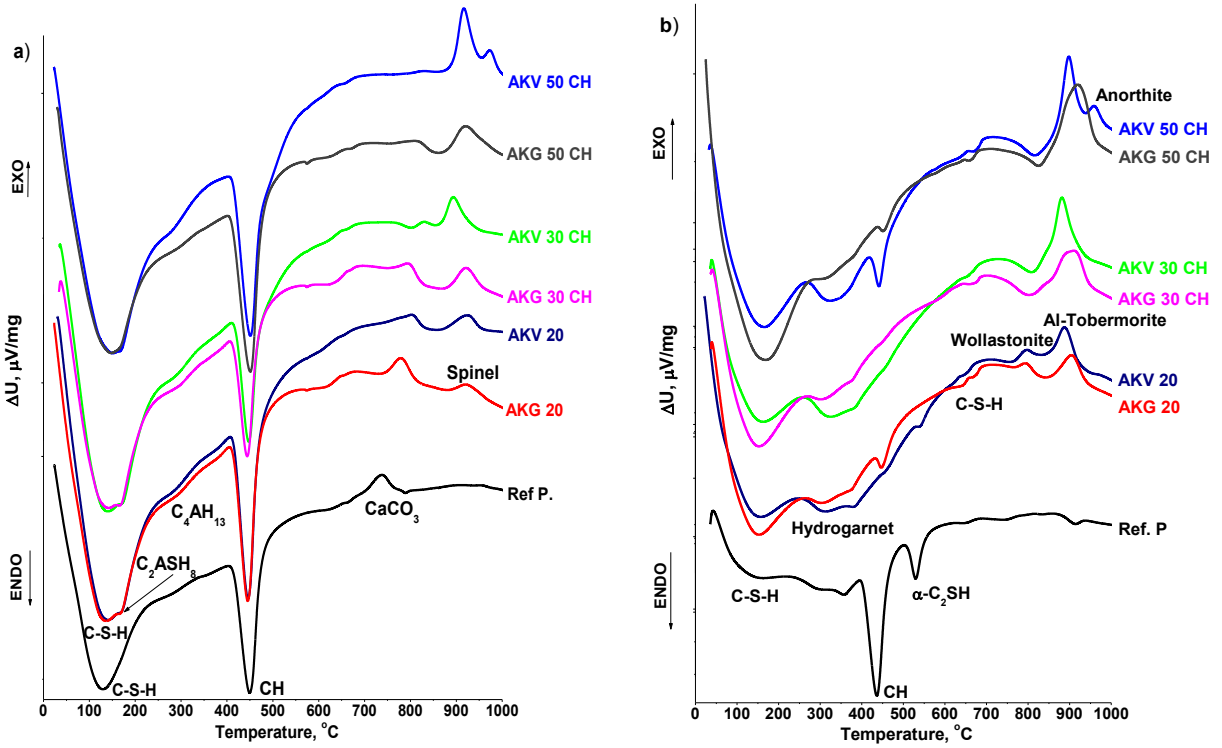

Fig. 3. DTA curves of pastes: a) ordinary cured at 28 days, b) autoclaved

A well-resolved peak at 530 °C, arising from dehydration of α-C_2SH, was recorded only for the reference paste. This peak completely vanished in AKV and AKG pastes.

Weak endotherm at ~650 °C, detected in all AKV and AKG pastes, arises from dehydration of other crystalline C-S-H phases [44]. The exotherm at 789 °C, may be attributed to the formation of wollastonite from the dehydration residues of C-S-H phases [28], while the exotherm at ~894 °C indicates reaction between α-C_2SH and either AKV or AKG, and appearance of Al-substituted tobermorite. The exotherm at ~960 °C, only detected in the AKV 50 CH paste, originated from the formation of anorthite.

These results confirmed XRD results (Fig. 2.) and gave us an explanation for higher AKG composite strengths. Namely, smaller content of hydrogarnet and higher content of C-S-H phase (strength-related phase) are responsible for higher compressive strength of AKG composites, compared to the AKV composites.

3.3.3 TG analyses

Following the DTA results, the mass loss of pastes (Fig. 4), both ordinary cured and autoclaved, may be arbitrary divided into four regions. The first (I), from 20 °C to 250 °C, mainly originates from dehydration of water chemically combined with hydrated phases present in the paste, including hydrated calcium silicate, strätlingite, ettringite et al. [48]. The second (II), between 250 °C and 400 °C, corresponds to decomposition of C-A-S-H phases, while for the autoclaved pastes it may be attributed to the hydrogarnet decomposition. The third region (III), approximately from 400 °C to 500 °C, originates from dehydroxilation of CH, while the fourth (IV), between 700 °C and 800 °C, is associated with decarbonation, as well as decomposition of C-S-H to wollastonite (as may be revealed at DTA curves at about 800 °C) [48].

The TG curves indicate that in the first and second region, mass loss was higher in AK pastes, compared to the reference, for both curing conditions (except the sample AKG 50 CH). It means that AKV and AKG substitution can increase the amount of hydration products (C-S-H and C-A-S-H phases) formed by pozzolanic reaction.

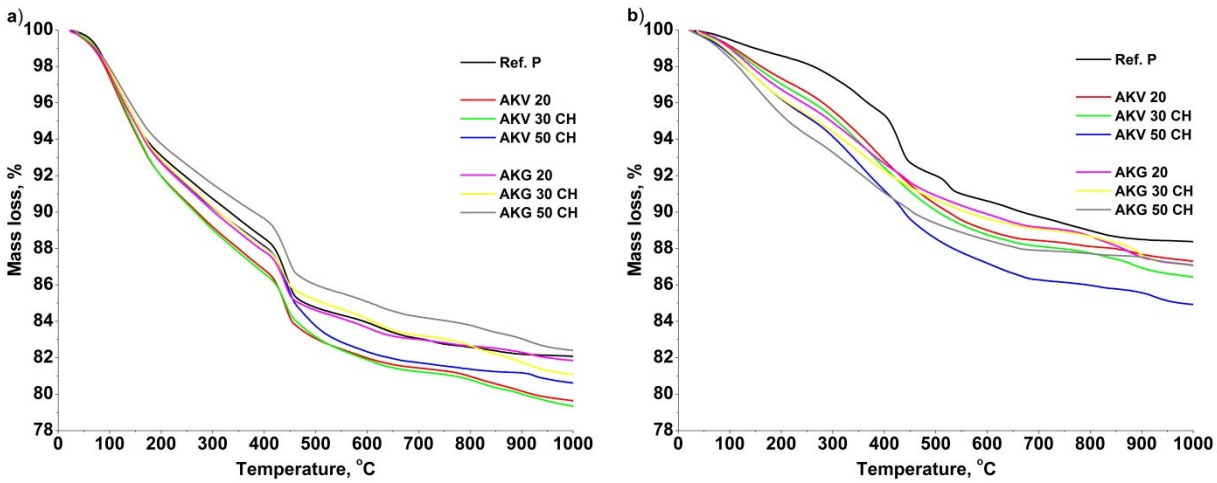

Fig. 4. TG curves of pastes: (a) ordinary cured at 28 days (b) autoclaved

As an attempt to correlate the compressive strength with pozzolanic reaction, portlandite (CH) consumed in pozzolanic reaction was estimated.

The free portlandite content (CH_f), formed during the hydration of pastes, was calculated by the following equation [40]:

$$CH_f(g) = \frac{\Delta m \times MM(CH) \times m_c}{MM(H_2O) \times 100} \quad (6)$$

where Δm is mass loss corresponds to the loss of H_2O in the dehydroxylation of CH, *MM*(CH) molecular mass of $Ca(OH)_2$, *MM*(H_2O) molecular mass of H_2O, and m_c cement content in paste. Mass loss was determined from TG analyses by stepwise method, as a difference between mass loss at temperatures T_{on} (onset) and T_{off} (end) related to the dehydroxilation of CH.

The content of CH consumed in the pozzolanic reaction (CH_c) was calculated according to equation [40]:

$$CH_c = CH_i - CH_f \quad (7)$$

where CH_i is the initial portlandite content in the corresponding paste (obtained by hydration of cement), including amount of CH added in the pastes with 30 and 50% of AKV and AKG, while CH_f is the free portlandite content calculated by Eq. (6). The results are presented in the Table 3.

Table 3. CH content in ordinary cured and autoclaved AKV and AKG pastes

	T_{on}, (°C)	T_{off}, (°C)	Δm, (%)	CH_f, (g)	CH_i, (g)	CH_c, (g)	CH_c, (%)
Ordinary cured							
AKV 20	407	507	3.75	61.7	64.1	2.4	3.8
AKG 20	406	501	3.13	51.5	64.1	12.6	19.7
AKV 30 CH	410	530	3.73	54.4	61.1	6.7	10.9
AKG 30 CH	406	500	2.77	40.4	61.1	20.7	33.9
AKV 50 CH	404	560	5.32	71.1	115.1	44.0	38.2
AKG 50 CH	400	515	3.80	50.8	115.1	64.3	55.9
Autoclaved							
AKV 20	445	464	0.48	7.9	56.6	48.7	86.0
AKG 20	434	473	0.75	12.3	56.6	44.3	78.2
AKV 30 CH	458	468	0.23	3.4	54.5	51.1	93.8
AKG 30 CH	-	-	-	0.0	54.5	54.5	100
AKV 50 CH	418	460	1.33	17.8	110.4	92.6	83.9
AKG 50 CH	438	488	0.83	11.1	110.4	99.3	90.0

The CH content in the ordinary cured reference paste was ~ 15.6% and in autoclaved ~ 13.7%.

For both, autoclaved and ordinary cured, AKG pastes consumed more CH in pozzolanic reaction, compared to the AKV pastes, except in the autoclaved paste AKG 20. Smaller consumption of CH in AKV pastes is a result of lower reactivity of AKV and the presence of non-amorphized kaolinite. Additionally, crystalline quartz from AKG at elevated temperature and pressure reacted with available CH according to Eq. 4. As a consequence of higher CH consumption, compressive strength of AKG composites was higher for all cement replacement levels, under the both curing conditions, compared to the AKV composites.

Comparing the influence of different curing conditions, it is evident that CH consumption was higher in autoclaved pastes, compare to the ordinary cured, indicating more pronounced pozzolanic reaction, which led to higher strengths.

3.4 Porosity and pore size distribution

The results of total porosity of pastes under the different curing conditions are shown in Table 4.

The total porosity of the autoclaved reference paste was nearly twice compared to the ordinary cured paste. It was a consequence of the formation of hydration products such as jaffeite, α-C_2SH, tobermorite and hydrogarnet [35], [36].

Table 4. Total porosity of ordinary cured and autoclaved AKV and AKG pastes

	Total porosity, %	
	Ordinary cured	Autoclaved
Ref.P	24.58	45.53
AKV 20	21.87	42.03
AKV 30 CH	21.12	41.22
AKV 50 CH	10.40	33.06
AKG 20	20.64	36.18
AKG 30 CH	20.52	36.38
AKG 50 CH	22.62	38.31

The total porosity of AKV and AKG pastes was lower than that of reference pastes, for both curing conditions. The results are in agreement with findings [49] that in most cases, mortars and concrete containing material with pozzolanic characteristics have (under ordinary conditions), porosity values equal to or inferior to that of OPC concrete. Porosity of the

pastes with 20% and 30%, of either AKV or AKG, were comparable for both curing conditions. Larger differences were obtained when 50% of mechanically activated kaolin replaced cement in the paste.

For AKV, porosity of the ordinary cured paste is about half, while in autoclaved paste the porosity decrease is less pronounced. Addition of 50% AKG, resulted in a small porosity increase, compared to pastes with 20% and 30% addition.

Addition of AKG and AKV led to the pore structure refinement, compared to the reference sample, as a consequence of the pozzolanic reaction, as it was shown in Fig. 5. Independent of curing conditions, AKG pastes had higher volume fraction of smaller pores, compared to the AKV pastes. It was especially pronounced under the autoclave curing.

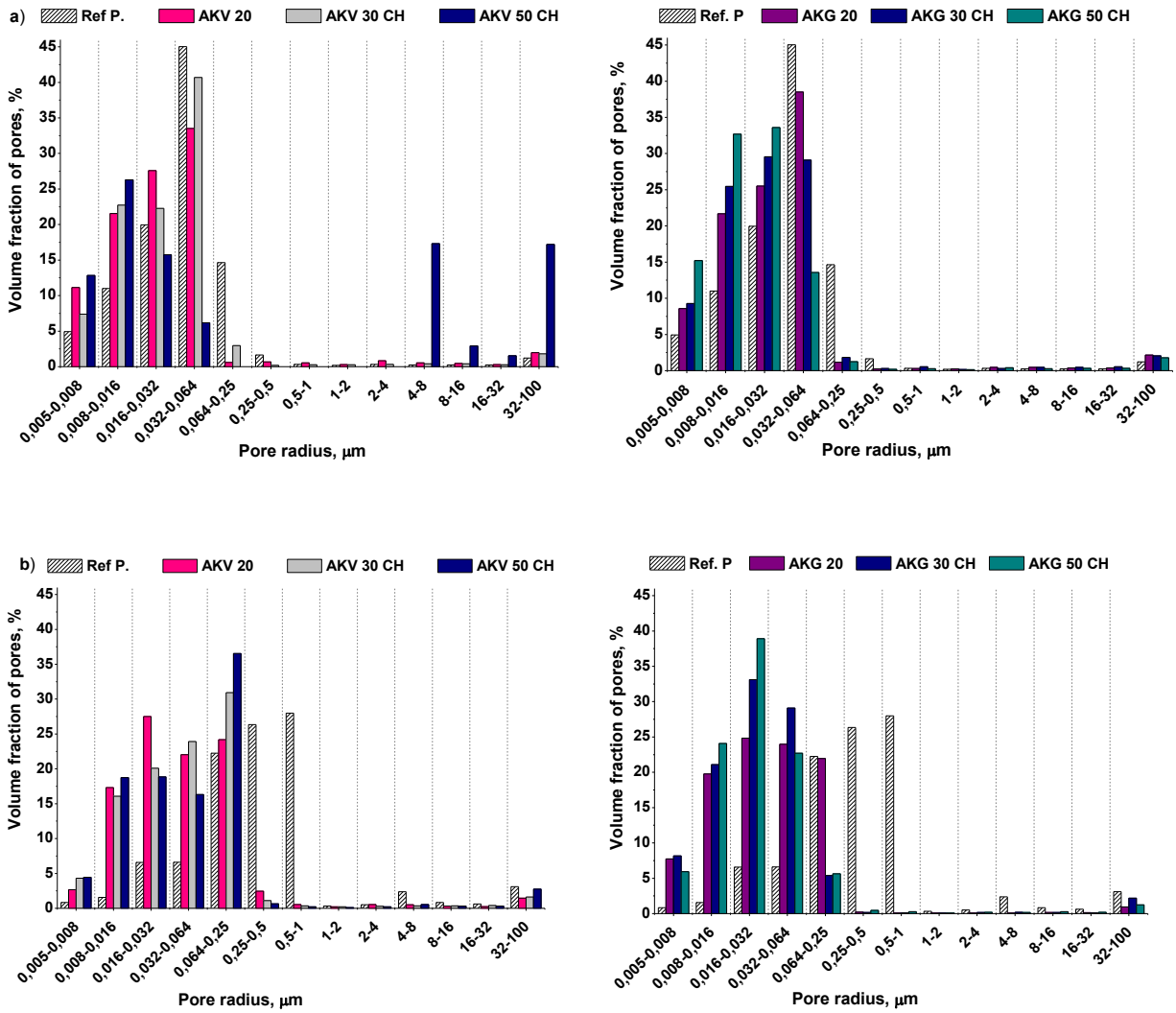

Fig.5. Pore size distribution of pastes (a) ordinary cured for 28 days (b) autoclaved

359 *3.5 SEM-EDS analysis*

360 In order to get more insight into the influence of the ordinary curing and autoclaving on the
361 properties of investigated composites, microstructure of the selected samples, namely,
362 reference, AKV 50 CH and AKG 50 CH pastes was examined by SEM-EDS analysis. *Možda*
363 *ubaciti ovu rečenicu:* Selected (*ili* Characteristic) images are presented in Figs. 6 and 7.
364 Figure 6 shows the SEM-EDS analyses of ordinary cured pastes. The primary structure of
365 the reference paste (Fig.6a) is formed of C-S-H phase with a spongy appearance and large
366 crystal plates of CH.
367 The SEM image of AKV 50 CH paste is presented in Fig. 6b. Randomly arranged, hexagonal
368 plate-like structure with broken edges, approximately larger than 20 μm in length, was
369 observed in the cavity (Fig.6b). The EDS analysis confirms that the formed product was the
370 tetracalcium aluminate hydrate (C_4AH_{13}), with calcium to aluminium (Ca/Al) ratio of 2.1.
371 Spherical pore filled with plate-formed, randomly oriented C-S-H phase were also detected
372 (SEM image not presented) and confirmed by EDS.
373 From the SEM image of AKG 50 CH paste (Fig. 6c) crystalline plate-like structure of C-S-H,
374 which was well embedded into the pore, was observed. The EDS analysis revealed calcium
375 to silicon (Ca/Si) ratio of approximately 1.5. Also, large crystalline of CH and hexagonal
376 plates forming crystal rods of CASH phases were also detected, but not presented. The EDS
377 analysis revealed that the structure was primarily composed of Ca, Al, Si and S. A firm
378 assertion of the phases involved is not possible, but plausible an intermixture of several
379 phases, like stratlingite and tetracalcium aluminate hydrate, as well as of
380 monosulfoaluminate appears. Trigonal crystals of quartz, originated from mechanically
381 activated kaolin, were also present all over the paste. The pore sizes were relatively smaller
382 in AKG 50 CH paste, compared to AKV paste, which was in agreement with the results of
383 pore size distribution (Fig. 5a).

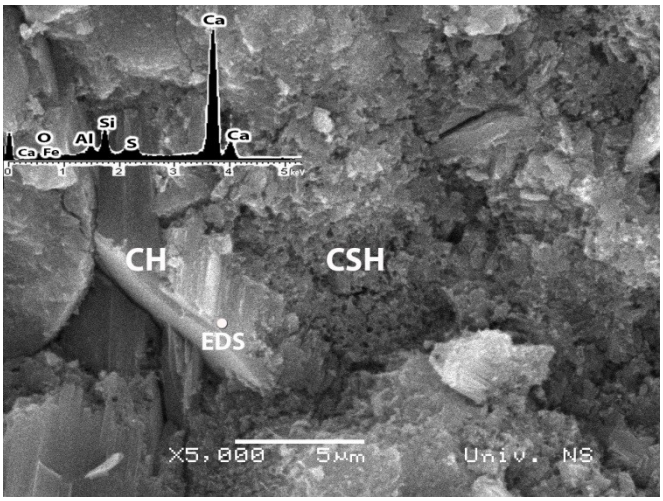

a) Ref. P

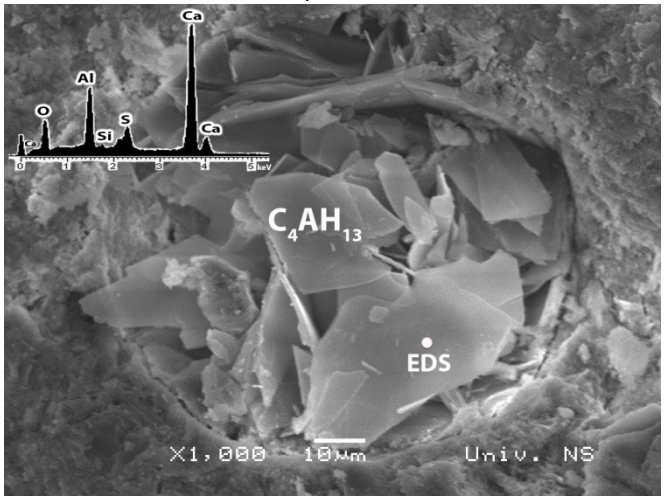

b) AKV 50 CH

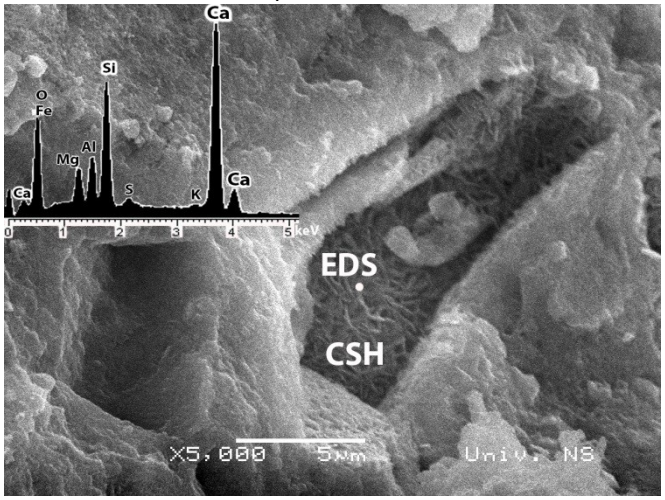

c) AKG 50 CH

384 Fig. 6 SEM - EDS analyses of ordinary cured pastes

385 Autoclaved pastes exhibited remarkably different morphology of hydration products in
386 comparison to ordinary cured. The SEM-EDS analysis of the autoclaved reference paste
387 is shown in Fig 7a. The acicular C-S-H phase was observed in the inner surface of the

388 cavity, while short needles, which turned into the plate-like and sponge structure, are
389 created at a rim of cavity. EDS analysis revealed that the formed product was jaffeite
390 ($C_3SH_{1,5}$) with Ca/Si ratio of 2.80. Large hexagonal plates of CH were also detected (SEM
391 image not presented).
392 The grassy porous structure of tobermorite, with long, bended strips, smaller than 1 μm in
393 width, was detected in AKV 50 CH paste (Fig. 7b). The EDS analysis revealed Ca/Si ratio
394 of 0.97. The presence of Al indicates its possible incorporation into the CSH lattice and
395 formation of Al-substituted tobermorite. Additionally, hydrogarnet agglomerates (C_3ASH_6)
396 with Ca/Si ratio of 3.15 and Ca/Al ratio of 1.43 was detected (SEM image not presented)
397 and confirmed by EDS.
398 Uniform and dense microstructure of plate-like tobermorite was observed through the
399 whole AKG 50 CH paste (Fig. 7 c). High peak intensities of Ca and Si observed on the
400 EDS spectra, confirmed formation of tobermorite. Considerably smaller Ca/Si ratio (0.75)
401 in comparison to the Ca/Si ratio (1.5) of ordinary cured AKG 50 CH paste, indicates that
402 the quartz reacted during autoclaving, while is normally non-reactive in ordinary curing
403 conditions [50]. According to the literature [39], [51] the formation of C-S-H phases with a
404 Ca/Si ratio of approximately unity is generally associated with high strength of
405 composites.
406 Morphology analysis showed quite good agreement with XRD results.

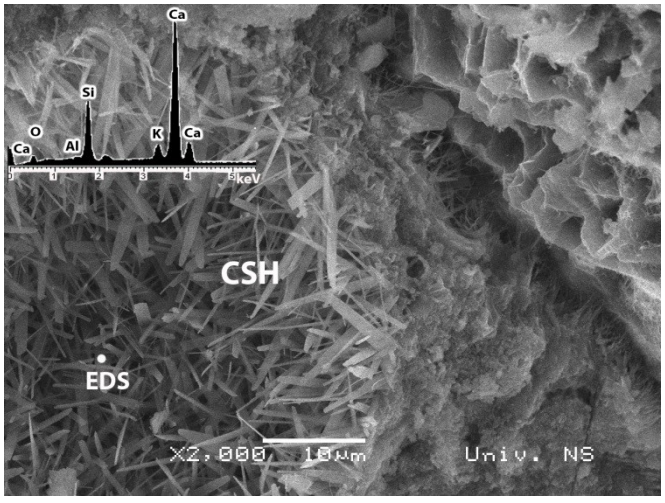

a) Ref. P

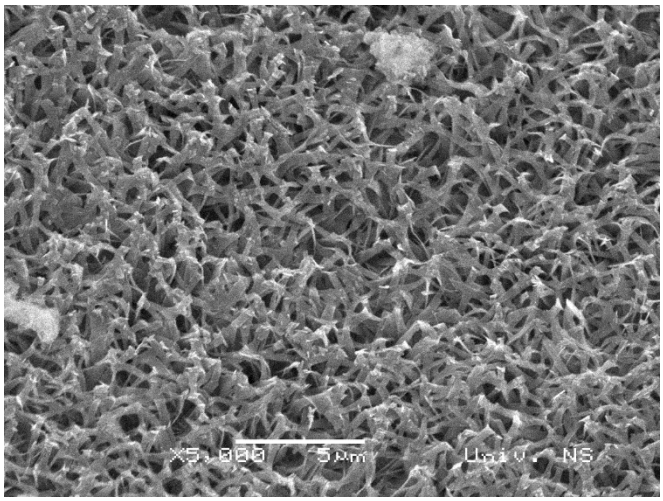

b) AKV 50 CH

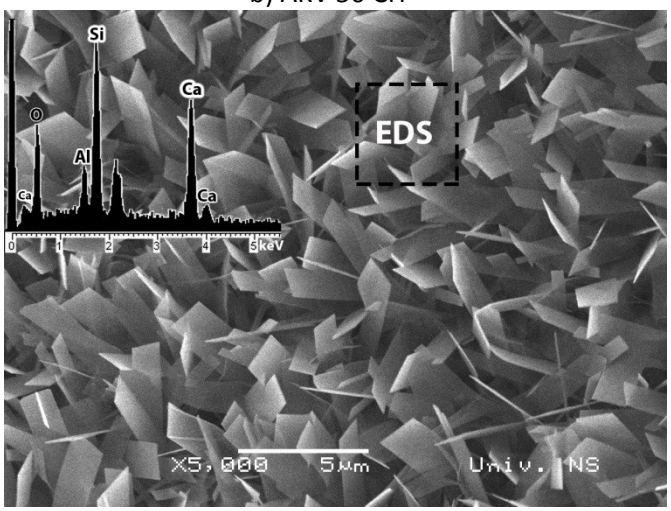

c) AKG 50 CH

Fig. 7 SEM-EDS analyses of autoclaved pastes

4. Conclusions

Composites with mechanically activated kaolin AKG, which contained high amount of quartz (~ 40%), attained higher compressive strengths for all cement replacement levels, under both curing conditions, compare to AKV. The strengths were considerable higher when autoclaving was applied, especially at higher cement replacement levels.

Analyzing microstructure of autoclaved AKG pastes, higher strengths could be explained by:

- higher CH consumption, which led to the more pronounced pozzolanic reaction and formation of higher C-S-H content;
- effects of finely milled quartz particles which reacted with portlandite and gave crystalline tobermorite (strength giving material) as the main reaction product, as well as their action as nuclei for the formation of new crystalline products;

- lower content of hydrogarnet;
- higher pore structure refinement.

Ordinary curing of composites caused substantial strength decrease as the cement replacement level increased, which was less pronounced with the addition of AKG.

Similar endothermic peaks that were attributed to the formation of C-S-H and CH phases in both AKV and AKG pastes were comparable to the reference, indicating weak pozzolanic reaction. Furthermore, significant lowering of the strengths is a main consequence of the dilution effect.

Slightly higher strengths obtained with ordinary cured AKG composites, compared to the AKV composites, mainly arised from the absence of kaolinite ~~peaks~~, which implies that a full amorphisation of kaolinite was succeed, as well as of higher CH consumption, which led to increased content of C-S-H phases. Additionally, AKG pastes had higher volume fraction of smaller pores, compared to the AKV pastes.

Acknowledgments

This work was financially supported by the Ministry of Education, Science and Technological Development of the Republic of Serbia (Grants Nos. TR 36017 and 45001).

References

[1] A. Moropoulou, A. Bakolas, E. Aggelakopoulou, Evaluation of pozzolanic activity of natural and artificial pozzolans by thermal analysis, Thermochim. Acta. 420 (2004) 135–140. doi:10.1016/j.tca.2003.11.059.

[2] S. Mohammed, Processing, effect and reactivity assessment of artificial pozzolans obtained from clays and clay wastes: A review, Constr. Build. Mater. 140 (2017) 10–19. doi:10.1016/j.conbuildmat.2017.02.078.

[3] B.B. Sabir, S. Wild, J. Bai, Metakaolin and calcined clays as pozzolans for concrete : a review, Cem. Concr. Compos. 23 (2001) 441–454. doi:10.1016/S0958-9465(00)00092-5.

[4] R. Siddique, J. Klaus, Influence of metakaolin on the properties of mortar and concrete: A review, Appl. Clay Sci. 43 (2009) 392–400.

447 doi:10.1016/j.clay.2008.11.007.
448 [5] A.M. Rashad, Metakaolin as cementitious material: History, scours, production and
449 composition – A comprehensive overview, Constr. Build. Mater. 41 (2013) 303–318.
450 doi:10.1016/j.conbuildmat.2012.12.001.
451 [6] G. Kakali, T. Perraki, S. Tsivilis, E. Badogiannis, Thermal treatment of kaolin: The
452 effect of mineralogy on the pozzolanic activity, Appl. Clay Sci. 20 (2001) 73–80.
453 doi:10.1016/S0169-1317(01)00040-0.
454 [7] E. Badogiannis, G. Kakali, S. Tsivilis, Metakaolin as supplementary cementitious
455 material : Optimization of kaolin to metakaolin conversion, J. Therm. Anal. Calorim. 81
456 (2005) 457–462. doi:10.1007/s10973-005-0806-3.
457 [8] C. Vizcayno, R.M. de Gutiérrez, R. Castello, E. Rodriguez, C.E. Guerrero, Pozzolan
458 obtained by mechanochemical and thermal treatments of kaolin, Appl. Clay Sci. 49
459 (2010) 405–413. doi:10.1016/j.clay.2009.09.008.
460 [9] M. Fitos, E.G. Badogiannis, S.G. Tsivilis, M. Perraki, Pozzolanic activity of thermally
461 and mechanically treated kaolins of hydrothermal origin, Appl. Clay Sci. 116–117
462 (2015) 182–192. doi:10.1016/j.clay.2015.08.028.
463 [10] B. Ilić, V. Radonjanin, M. Malešev, M. Zdujić, A. Mitrović, Effects of mechanical and
464 thermal activation on pozzolanic activity of kaolin containing mica, Appl. Clay Sci. 123
465 (2016) 173–181. doi:10.1016/j.clay.2016.01.029.
466 [11] A. Souri, H. Kazemi-Kamyab, R. Snellings, R. Naghizadeh, F. Golestani-Fard, K.
467 Scrivener, Pozzolanic activity of mechanochemically and thermally activated kaolins in
468 cement, Cem. Concr. Res. 77 (2015) 47–59. doi:10.1016/j.cemconres.2015.04.017.
469 [12] E. Horvath, R.L. Frost, E. Mako, J. Kristof, T. Cseh, Thermal treatment of
470 mechanochemically activated kaolinite, Thermochim. Acta. 404 (2003) 227–234.
471 doi:10.1016/S0040-6031(03)00184-9.
472 [13] F. Gonzalez Garcia, Effects of dry grinding on two kaolins of different degrees of
473 crystallinity, Clay Miner. 26 (1991) 549–565. doi:10.1180/claymin.1991.026.4.09.
474 [14] P.J. Sanchez-Soto, M. Del Carmen Jimenez de Haro, L.A. Perez-Maqueda, I. Varona,

475 J.L. Perez-Rodriguez, Effects of dry grinding of kaolinite, J. Am. Ceram. Soc. 83
476 (2000) 1649–1657.
477 [15] E.F. Aglietti, J.M.P. Lopez, E. Pereira, Mechanochemical effects in kaolinite grinding.
478 ii. structural aspects, Int. J. Miner. Process. 16 (1986) 135–146.
479 [16] R. Siddique, M. Iqbal Khan, Supplementary Cementing Materials, Springer-Verlag
480 Berkin Heidelberg, 2011. doi:10.1007/978-3-642-17866-5.
481 [17] A.M. Rashad, Metakaolin: Fresh properties and optimum content for mechanical
482 strength in traditional cementitious materials - A comprehensive overview, Rev. Adv.
483 Mater. Sci. 40 (2015) 15–44.
484 [18] F. Cassagnabère, M. Mouret, G. Escadeillas, P. Broilliard, A. Bertrand, Metakaolin, a
485 solution for the precast industry to limit the clinker content in concrete: Mechanical
486 aspects, Constr. Build. Mater. 24 (2010) 1109–1118.
487 doi:10.1016/j.conbuildmat.2009.12.032.
488 [19] F. Cassagnabère, M. Mouret, G. Escadeillas, Early hydration of clinker-slag-
489 metakaolin combination in steam curing conditions, relation with mechanical
490 properties, Cem. Concr. Res. 39 (2009) 1164–1173.
491 doi:10.1016/j.cemconres.2009.07.023.
492 [20] B. Ilić, V. Radonjanin, M. Malešev, M. Zdujić, A. Mitrović, Study on the addition effect
493 of metakaolin and mechanically activated kaolin on cement strength and
494 microstructure under different curing conditions, Constr. Build. Mater. 133 (2017) 243–
495 252. doi:10.1016/j.conbuildmat.2016.12.068.
496 [21] R. Hamzaoui, S. Guessasma, A. Bennabi, Kaolinite obtained by ball milling as a
497 potential substituent for cement : mechanical performance effect on mortar based
498 cement and milled kaolinite, in: Int. Conf. Innov. Constr., Paris, 2015.
499 [22] Lj. Miličić, A. Mitrović, M. Zdujić, D. Nikolić, Strengths of the mortars containing
500 amorphous kaolin as cement replacement material, in: 5th Int. Conf. Civ. Eng. - Sci.
501 Pract., Žabljak, 2014: pp. 971–976.
502 [23] A. Mitrović, Lj. Miličić, M. Zdujić, Amorphous kaolin as cement replacement material,

in: Int. Conf. „Contemporary Achiev. Civ. Eng. 2014“, Subotica, 2014: pp. 483–488. doi:10.14415/konferencijaGFS2014.

[24] A. Mitrović, M. Zdujić, Preparation of pozzolanic addition by mechanical treatment of kaolin clay, Int. J. Miner. Process. 132 (2014) 59–66. doi:10.1016/j.minpro.2014.09.004.

[25] M. Murat, Hydration reaction and hardening of calcined clays and related minerals. I. Preliminary investigation on metakaolinite, Cem. Concr. Res. 13 (1983) 259–266. doi:10.1016/0008-8846(83)90109-6.

[26] K. Luke, Phase studies of pozzolanic stabilized calcium silicate hydrates at 180 °C, Cem. Concr. Res. 34 (2004) 1725–1732. doi:10.1016/j.cemconres.2004.05.021.

[27] H. Yazici, The effect of curing conditions on compressive strength of ultra high strength concrete with high volume mineral admixtures, Build. Environ. 42 (2007) 2083–2089. doi:10.1016/j.buildenv.2006.03.013.

[28] A.C. Jupe, A.P. Wilkinson, K. Luke, G.P. Funkhouser, Class H cement hydration at 180 °C and high pressure in the presence of added silica, Cem. Concr. Res. 38 (2008) 660–666. doi:10.1016/j.cemconres.2007.12.004.

[29] Q. Yang, S. Zhang, S. Huang, Y. He, Effect of ground quartz sand on properties of high-strength concrete in the steam-autoclaved curing, Cem. Concr. Res. 30 (2000) 1993–1998.

[30] M. Ashraf, A.N. Khan, Q. Ali, J. Mirza, A. Goyal, A.M. Anwar, Physico-chemical, morphological and thermal analysis for the combined pozzolanic activities of minerals additives, Constr. Build. Mater. 23 (2009) 2207–2213. doi:10.1016/j.conbuildmat.2008.12.008.

[31] D.S. Klimesch, A. Ray, The use of DTA/TGA to study the effects of ground quartz with different surface areas in autoclaved cement : Quartz pastes. Part 1: A method for evaluating DTA/TGA results, Thermochim. Acta. 289 (1996) 41–54. doi:10.1016/S0040-6031(96)03033-X.

[32] W. Sha, E. a. O'Neill, Z. Guo, Differential scanning calorimetry study of ordinary

531 Portland cement, Cem. Concr. Res. 29 (1999) 1487–1489. doi:10.1016/S0008-
532 8846(99)00128-3.
533 [33] B. Ilić, V. Radonjanin, M. Malešev, M. Zdujić, A. Mitrović, Effects of mechanical and
534 thermal activation on pozzolanic activity of kaolin containing mica, Appl. Clay Sci. 123
535 (2016) 173–181. doi:10.1016/j.clay.2016.01.029.
536 [34] M. Cyr, M. Trinh, B. Husson, G. Casaux-Ginestet, Effect of cement type on metakaolin
537 efficiency, Cem. Concr. Res. 64 (2014) 63–72. doi:10.1016/j.cemconres.2014.06.007.
538 [35] S. Mindess, F. Young, D. Darwin, Concrete, 2nd ed., Prentice Hall, Pearson
539 Education, Inc. New Jersey, 2002.
540 [36] H.F.W. Taylor, Cement Chemistry, Academic Press, London, 1990.
541 [37] C. Shi, S. Hu, Cementitious properties of ladle slag fines under autoclave curing
542 conditions, Cem. Concr. Res. 33 (2003) 1851–1856. doi:10.1016/S0008-
543 8846(03)00211-4.
544 [38] M.S. Amin, S.A. Abo-El-Enein, A. Abdel Rahman, K.A. Alfalous, Artificial pozzolanic
545 cement pastes containing burnt clay with and without silica fume, J. Therm. Anal.
546 Calorim. 107 (2012) 1105–1115. doi:10.1007/s10973-011-1676-5.
547 [39] O.A. Alawad, A. Alhozaimy, M.S. Jaafar, A. Al-Negheimish, F.N.A. Aziz,
548 Microstructure analyses of autoclaved ground dune sand–Portland cement paste,
549 Constr. Build. Mater. 65 (2014) 14–19. doi:10.1016/j.conbuildmat.2014.04.040.
550 [40] A. Gameiro, A. Santos Silva, R. Veiga, A. Velosa, Hydration products of lime-
551 metakaolin pastes at ambient temperature with ageing, Thermochim. Acta. 535 (2012)
552 36–41. doi:10.1016/j.tca.2012.02.013.
553 [41] M. Frías, J. Cabrera, Influence of MK on the reaction kinetics in MK/lime and MK-
554 blended cement systems at 20 °C, Cem. Concr. Res. 31 (2001) 519–527.
555 [42] M. Murat, Hydratation reaction and hardening of calcined clays and related minerals.
556 Influence of mineralogical properties of the raw-kaolinite on the reactivity of
557 metakaolinite, Cem. Concr. Res. 13 (1983) 511–518.
558 [43] F. Cassagnabère, G. Escadeillas, M. Mouret, Study of the reactivity of

559 cement/metakaolin binders at early age for specific use in steam cured precast
560 concrete, Constr. Build. Mater. 23 (2009) 775–784.
561 doi:10.1016/j.conbuildmat.2008.02.022.
562 [44] D.S. Klimesch, A. Ray, Use of the second-derivative differential thermal curve in the
563 evaluation of cement-quartz pastes with metakaolin addition autoclaved at 180 °C,
564 Thermochim. Acta. 307 (1997) 167–176.
565 [45] O.A. Alawad, A. Alhozaimy, M.S. Jaafar, F. Nora, A. Aziz, A. Al-Negheimish, Effect of
566 autoclave curing on the microstructure of blended cement mixture incorporating
567 ground dune sand and ground granulated blast furnace slag, Int. J. Concr. Struct.
568 Mater. 9 (2015) 381–390. doi:10.1007/s40069-015-0104-9.
569 [46] D.S. Klimesch, A. Ray, DTA–TGA of unstirred autoclaved metakaolin–lime–quartz
570 slurries. The formation of hydrogarnet, Thermochim. Acta. 316 (1998) 149–154.
571 doi:10.1016/S0040-6031(98)00307-4.
572 [47] M.F. Rojas, M.I. Sánchez de Rojas, The effect of high curing temperature on the
573 reaction kinetics in MK/lime and MK-blended cement matrices at 60 °C, Cem. Concr.
574 Res. 33 (2003) 643–649. doi:10.1016/S0008-8846(02)01040-2.
575 [48] K. Scrivener, R. Snellings, B. Lothenbach, A Practical Guide to Microstructural
576 Analysis of Cementitious Materials, CRC Press Taylor & Francis Group, 2016.
577 doi:10.7693/wl20150205.
578 [49] M. Frías, J. Cabrera, Pore size distribution and degree of hydration of metakaolin-
579 cement pastes, Cem. Concr. Res. 30 (2000) 561–569. doi:10.1016/S0008-
580 8846(00)00203-9.
581 [50] H. Yazici, E. Deniz, B. Baradan, The effect of autoclave pressure, temperature and
582 duration time on mechanical properties of reactive powder concrete, Constr. Build.
583 Mater. 42 (2013) 53–63. doi:10.1016/j.conbuildmat.2013.01.003.
584 [51] A.C. Jupe, A.P. Wilkinson, K. Luke, G.P. Funkhouser, Class H cement hydration at
585 180 °C and high pressure in the presence of added silica, Cem. Concr. Res. 38 (2008)
586 660–666. doi:10.1016/j.cemconres.2007.12.004.

587